THE JOURNAL OF PHYSICAL CHEMISTRY B

Article

pubs.acs.org/JPCB

Laser-Heating-Induced Displacement of Surfactants on the Water Surface

Ellen H. G. Backus,*[,†] Daniel Bonn,[‡] Sophie Cantin,[§] Sylvie Roke,[∥] and Mischa Bonn[†,⊥]

[†]FOM Institute AMOLF, Science Park 104, 1098 XG Amsterdam, The Netherlands

[‡]Laboratoire de Physique Statistique de l'ENS, 24 Rue Lhomond, F-75231 Paris cedex 05, France

[§]Laboratoire de Physico-Chimie des Polymères et des Interfaces (LPPI, EA 2528), Institut des matériaux, Université de Cergy-Pontoise, 5 mail Gay-Lussac Neuville/Oise, 95031 Cergy-Pontoise Cedex, France

[∥]Laboratory for Fundamental Biophotonics (LBP), Institute of Bioengineering, School of Engineering, École Polytechnique Fédérale de Lausanne, 1015 Lausanne, Switzerland

[⊥]Max-Planck Institute for Polymer Research, Ackermannweg 10, 55128 Mainz, Germany

ABSTRACT: We report a combined vibrational sum-frequency generation (SFG) spectroscopy, Brewster angle microscopy (BAM), and ellipsometry study of different surfactants on water as a function of surfactant density. Vibrational SFG spectra of surfactants on the water surface in a Langmuir trough have been measured in both the surfactant CH and the water OH stretch regions. At low densities, the SFG signal generated at the surface in the presence of the surfactant is indistinguishable from the SFG signal generated at the clean water−air interface. When the surfactant density increases, i.e., upon compressing the monolayer, a very sudden increase in the SFG signal in both the CH and OH spectral regions is observed. For higher laser fluences, this stepwise increase occurs at increasingly higher surfactant densities. Since BAM shows that surfactant molecules are clearly present at these low densities, we conclude that at low surfactant density the laser beam displaces relatively high-density domains with surfactants in the liquid expanded phase out of the region of the laser focus. This is a consequence of the thermal gradient induced by local heating of the water phase with the monolayer on top due to repetitive laser excitation at 1 kHz. It can be circumvented by using a rotating trough. In this manner, the sampled surface area can be refreshed, allowing artifact-free vibrational SFG spectra to be measured down to the very lowest surfactant densities. In ellipsometry experiments, a similar step can be noticed, which, however, is of a different nature; i.e., it is not related to heating (the laser fluence is very low and the light nonresonant) but to a molecular transition. The occurrence of the step in ellipsometry as a function of area per molecule depends critically on the preparation of the monolayer. By giving the molecules time and space to relax during the preparation of the monolayer, this step could also be eliminated.

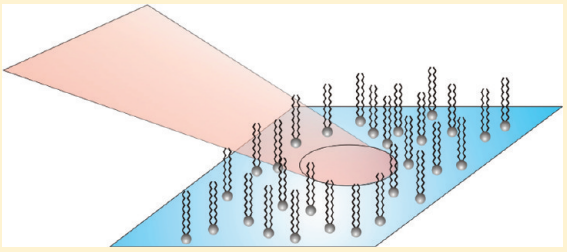

INTRODUCTION

In the last decades, infrared-visible sum-frequency generation (SFG) has been shown to be an excellent tool to study surfactants on an aqueous subphase.[1−9] In this technique, an infrared laser beam is combined with a visible laser beam at the interface of interest, and the sum-frequency beam of the two is detected. The generation of a signal is generally forbidden in centrosymmetric media and therefore sensitive to the presence of molecules at the interface. The SFG intensity is enhanced if the infrared laser is in resonance with a vibrational transition of molecules at the interface, so that the vibrational spectrum of the interfacial molecules can be measured. The shape of the SFG spectrum contains information about the molecular conformation and orientation of the surfactants. Most research has focused on high density monolayers, although at low density surprising observations have been reported. Some of us (Roke et al.[4]) have previously reported the appearance and disappearance of the signal of the C−H stretch modes of the insoluble surfactant DPPC (1,2-dipalmitoyl-*sn*-glycero-3-phosphocholine; see Figure 1) on water at a density around 100 Å^2 per molecule over a density interval of less than 1 Å^2 per molecule, which was attributed to curling and uncurling of the lipid tails. Recently, Chen et al.[9] reported similar behavior around this density for the CH signal from DPPC on water and on water containing a low molar fraction of DMSO. Moreover, they report that the signal from the P═O vibration originating from the headgroup of DPPC only appears if a CH signal is present. They assign the absence/presence of the CH signal to disordered/ordered tails of the DPPC molecules. The absence of the P═O signal was explained by a large orientational distribution of the headgroup.

While these explanations are consistent with the data, it is perhaps somewhat surprising that the lipid signal disappears for all modes; even for a highly disordered monolayer in which the

Received: August 4, 2011
Revised: February 6, 2012
Published: February 10, 2012

   dx.doi.org/10.1021/jp2074545 | *J. Phys. Chem. B* 2012, 116, 2703−2712

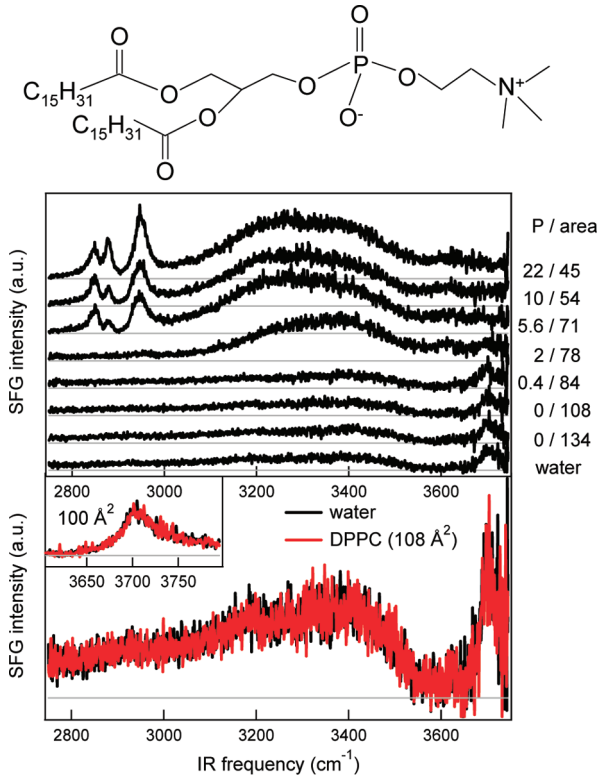

Figure 1. Top panel: Molecular structure of DPPC. Middle panel: SFG spectra in SSP polarization for a bare water surface (bottom spectrum) and for DPPC on water with increasing density. The pressure (mN/m) and area per molecule (Å^2), increasing and decreasing, respectively, from bottom to top are given next to the graph. The area per molecule has been controlled by the amount of droplets of chloroform solution. CH (2800−3000 cm^{-1}), H-bonded OH (3000−3600 cm^{-1}), and the free OH (∼3705 cm^{-1}) stretch vibration are visible. Bottom panel: An enlargement from the middle panel of the bare water surface and the one with DPPC at 108 Å^2 per molecule to indicate their similarity. The inset enlarges the free OH stretch vibration region for a bare water surface and one with DPPC (100 Å^2). At this area per molecule, the pressure is still below the detection limit, and the presence of DPPC at the surface apparently does not affect the amplitude of the free OH stretch vibration. A relatively high IR fluence (∼10 mJ/cm^2) is used for this experiment.

lipids are curled up, the symmetry is broken, if only because of the different dielectric constants of water and air at the two sides of the (possibly centrosymmetric) lipid layer. Both Roke et al. and Chen et al. base their conclusions on SFG spectra in the C−H and P═O stretch region, i.e., on modes originating from the lipid. The hydrogen-bonded water signal has not been investigated before and would bring more insight into the observed phenomenon. One might expect that the water signal can also contribute to the understanding of the organization of lipids if the density is changing. In particular, the question presents itself how the water structure is affected by the possibly disordered lipids. The signal of the hydrogen-bonded water at the water−air interface is generally larger if surfactants are present, where the strength of the water SFG signal depends on the type of surfactant.[10−12] Therefore, upon compressing a lipid layer changes in the water band are expected. Moreover, the free OH is expected to be affected upon compressing the monolayer, as was seen before for the free OD.[13] Here, we measure simultaneously the surfactant and the water molecules for a monolayer of DPPC at various densities. In a conventional SFG experiment, in which the sample reservoir is fixed, with increasing lipid density, a stepwise transition occurs from a spectrum that is indistinguishable from that of the water−air interface to one with a more intense water spectrum and CH modes present. The intensity step observed in the water spectrum correlates perfectly with the CH signal originating from the surfactant. When the sample reservoir is continuously moved, this intensity step is absent.

By using Brewster Angle Microscopy (BAM), we will show that although the surfactant is invisible with SFG it is really present at the surface already at very low density. BAM is very suitable to visualize domains of surfactant of relatively high density on a water surface. At the Brewster Angle (∼53° for water with a HeNe laser), the reflection of p polarized light vanishes. However, if surfactant or lipid domains are present on the surface, they can be visualized since they do reflect some of the light at the Brewster angle.

Here, we investigate to what extent the observed discontinuity in the SFG signal is induced by the way in which the measurement is performed. We find that SFG can be invasive under certain conditions: at low surfactant densities (i.e., area per molecule > 100 Å^2), the repetitive heating of the water surface layer by the resonant infrared (IR) laser pulses gives rise to high-density surfactant domains being displaced from the laser focus due to flow induced by the thermal gradient. At higher average surfactant densities, the laser-induced thermal gradient is no longer sufficient to keep the domains out of the laser focus, and the signal abruptly increases. This explains the discontinuity in SFG signals previously observed for monolayers at low densities. To generalize our conclusions, we show that this behavior is not only observed for monolayers of lipids but also for other surfactant types. We investigate a fatty acid (palmitic acid) and an alcohol (1-dodecanol). Moreover, we report the true noninvasive SFG spectra for DPPC on water from very low density (∼300 Å^2 per molecule) to high density (∼50 Å^2 per molecule) by using a rotating trough. These new results show very gradual increase in the SFG signals.

Surprisingly, also in the coefficient of ellipticity obtained by performing ellipsometry, a similar step at low density has often been observed for lipids and fatty acids.[14−18] Ellipsometry is basically the spatially integrated version of BAM; i.e., instead of a two-dimensional picture the coefficient of ellipticity is obtained. We submit that the intensity step observed for ellipsometry is of a different origin than the step in SFG. Heating of the monolayer is negligible, because in ellipsometry the laser is not resonant with water and the fluence is low. We find that for ellipsometry, in contrast to SFG, the step is dependent on the sample preparation. By giving the molecules time and space to relax we could also eliminate this step.

■ EXPERIMENTAL SECTION

For the SFG experiment, broad band infrared pulses (fwhm of ∼200 cm^{-1}) were generated by an OPG/OPA (TOPAS, Light Conversion) pumped by ∼1 W of 800 nm pulses from a Coherent Legend laser system (1 kHz, ∼120 fs fwhm). In parallel, ∼0.5 W of the laser output is passed through an etalon generating the narrow band VIS pulse (12 490 cm^{-1}, ∼30 μJ, fwhm bandwidth of ∼15 cm^{-1}) to provide the spectral resolution of the experiment. The broad band IR pulse allows the detection of a multitude of vibrational modes at once. The infrared pulse is centered at ∼3100 cm^{-1} (∼6 μJ) for the

dx.doi.org/10.1021/jp2074545 | J. Phys. Chem. B 2012, 116, 2703−2712

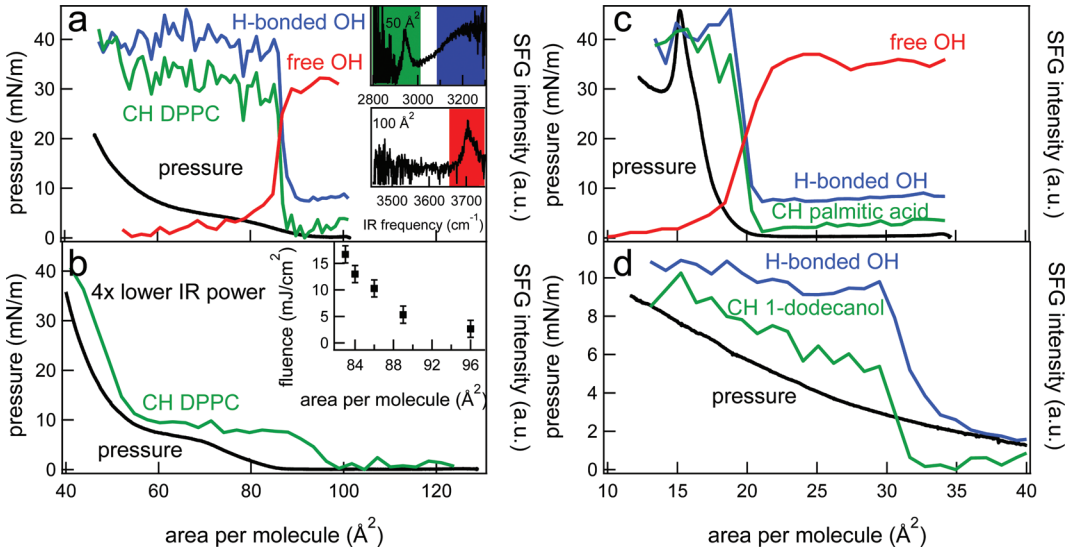

Figure 2. (a) Surface pressure (black, left axis) and integrated SFG intensity (right axis) for the CH signal of DPPC (green), the H-bonded OH signal (blue), and the free OH signal (red) as a function of the area per molecule during continuously compressing the monolayer. The integrated SFG signals are normalized and have a small offset with respect to each other for clarity. The integrated spectral areas are marked by the colored squares in the insets showing the SFG spectra for 50 and 100 Å^2 per molecule in the CH/OH-bonded and free OH region, respectively. A relatively high IR fluence (~10 mJ/cm^2) has been used. (b) Like (a), but with a four times lower IR power resulting in a four times lower fluence (~2.5 mJ/cm^2). The inset shows the effect of changing the IR fluence on the area per molecule where the SFG signal appears. (c) Like (a), but for palmitic acid. (d) Like (a), but for 1-dodecanol. The free OH was not measured in this case for 1-dodecanol. The SFG results are obtained under SSP polarization.

experiments in which the CH and hydrogen bonded OH vibration are detected and at ~3700 cm^{-1} (~3 μJ) for the free OH experiment. For some experiments, the IR center frequency was continuously varied ("swept") between 2750 and 3750 cm^{-1} to measure the CH and full OH region on the same time. It took roughly a minute to cycle from 2750 to 3750 and back to 2750 cm^{-1}. The incident angles of the VIS and IR beam were, respectively, ~35° and ~40° with respect to the surface normal. The VIS beam was focused down to approximately 400 μm beam waist. The IR focus was changed in between experiments. Most experiments were performed with an IR focus size of ~200 μm Gaussian beam waist, resulting in a fluence of ~10 mJ/cm^2. For the low fluence (~1.5 mJ/cm^2) experiments (Figures 5 and 7, top panel), we moved the IR lens so that the beam waist at the sample was ~500 μm. The SFG light was spectrally dispersed by a monochromator and detected by an Electron-Multiplied Charge Coupled Device (EMCCD, Andor Technologies). During monolayer compression SFG spectra were continuously measured with an acquisition time of 30 s for each spectrum with a fixed IR frequency. An acquisition time of 6 (high fluence) or 10 (low fluence) min was used for the experiments where the IR frequency was scanned between 2750 and 3750 cm^{-1}. The SFG spectra are recorded under s-polarized SFG, s-polarized VIS, and p-polarized IR conditions (SSP) unless stated otherwise and are normalized to a reference spectrum taken from z-cut quartz.

For the Brewster Angle Microscopy (BAM), a home-built machine was used equipped with a 50 mW 532 nm laser.[19] The p-polarized light was reflected off the surface at approximately the Brewster angle (~53°) and received by a microscope. As the monolayer was inclined on the visualization axis, the image was in focus only on a narrow strip. To obtain a sufficiently large image, the images of different strips formed by focusing at different levels on the monolayer were then placed side by side. Large images of 600 μm × 600 μm were thus obtained, with a spatial resolution close to 1 μm.

Ellipsometry measurements were performed using two different ellipsometers. One was a home-built polarization modulated machine working at the Brewster angle (~53°) and equipped with a laser that produced 5 mW 632 nm light. The other one was a commercial null ellipsometer (Optrell) with a 2 mW 632 nm laser incident under an angle of 50°. For both ellipsometry and BAM, the illuminated area amounted to a few square millimeters.

The surfactants DPPC (1,2-dipalmitoyl-*sn*-glycero-3-phosphocholine), 1-dodecanol ($C_{12}H_{25}OH$), and palmitic acid ($C_{15}H_{31}COOH$) were obtained from Avanti Polar Lipids, Fluka, and Sigma-Aldrich, respectively, and were used without further purification. Monolayers were spread from a chloroform solution (DPPC ~0.5 mM, 1-dodecanol ~3 mM, palmitic acid ~2 mM) on an air−H_2O (Millipore, 18 MΩ cm) interface. Monolayers with varying surface density were prepared in two ways: the area per molecule was controlled either through the number of 0.5 μL droplets spread on the water surface or by compressing the layer. The surface pressure was measured with a commercial (Kibron Inc., Finland) tensiometer using a needle. As the ellipsometry results depend on the manner of monolayer preparation, we provide an explicit description of the preparation for each type of experiment.

SFG. In the experiments where we swept the IR frequency continuously to obtain the whole CH and OH spectrum at once, a home-built 7 × 7 cm^2 Teflon-coated trough was used (Figure 1 and Figure 7, bottom panel). For the experiments for which the sample is (partially) refreshed between laser shots, a home-built, circular (8 cm diameter) Teflon trough was used (Figures 5 and 6). This trough was rotated using a simple 12 V DC electromotor driving a home-built rotation stage in such a manner that at the laser focus the sample moves with a speed of ~0.06 m/s. In both cases the area per molecule was controlled

dx.doi.org/10.1021/jp2074545 | J. Phys. Chem. B 2012, 116, 2703−2712

by the number of 0.5 μL droplets spread on the water surface. For experiments that required a high resolution for the area per molecule (Figure 2), we used a commercial metal Langmuir trough of 6 × 23 cm (Kibron Inc., Finland). The layer was compressed with one barrier with a speed between 5 and 10 mm/min (~1.3−2.6 Å^2/chain/min). The initial area per molecule was controlled by the number of 0.5 μL droplets of a solution of surfactant in chloroform.

BAM. In the Brewster Angle Microscopy (BAM) experiments (Figure 3), a Teflon trough with an area of 324 cm^2 was used. After depositing droplets of solution such that the area per molecule was 150 Å^2 per molecule, the density of the layer was controlled by compressing the monolayer with one barrier. At certain densities, the barrier was stopped to collect images.

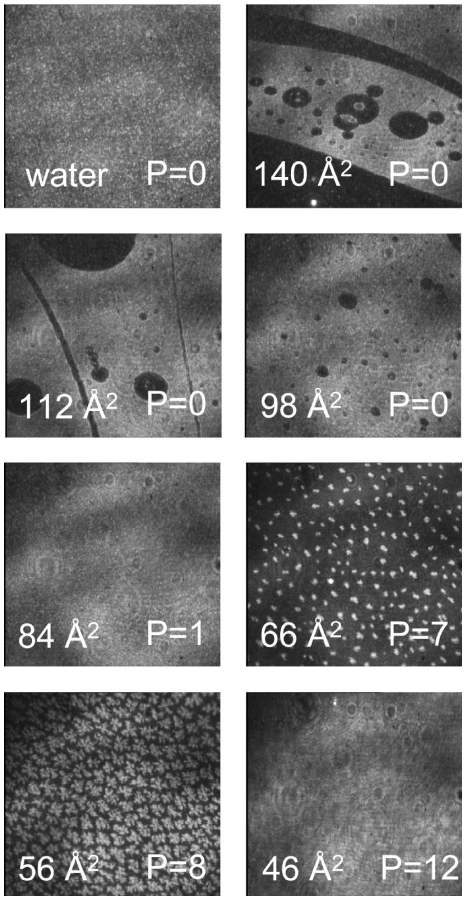

Figure 3. Brewster Angle Microscopy images for different densities of DPPC on water. The image size is 600 × 600 μm. White regions indicate high density, while black indicates low density. In every panel the area per molecule (in Å^2) is reported in the bottom left corner and the surface pressure (in mN/m) in the bottom right corner. The pictures are taken with a camera that automatically adjusts its sensitivity, so that the intensity gray scales cannot be compared between images.

Ellipsometry. In one set of experiments, the surface area was controlled, after initially depositing droplets of a chloroform solution, by compressing the layer with a speed of 5 mm/min in a commercial metal Langmuir trough of 6 × 23 cm (Kibron Inc., Finland) with one barrier (Figure 8a and 8c). In another experiment, the area per molecule was controlled by the number of 0.5 μL droplets spread on the water surface in a home-built round (8 cm diameter) Teflon-coated trough (Figure 8b). As shown below, different results can be obtained for monolayers prepared in different manners.

RESULTS AND DISCUSSION

In the following, we will present SFG experiments on a static monolayer, which shows anomalous, stepwise intensity variations of the SFG signals. In contrast, BAM microscopy images reveal a homogeneous monolayer on the length scales of the SFG experiments. By reducing the fluence, or continuously moving the monolayer during the SFG experiment, the true SFG response of the monolayer can be recorded. Finally, ellipsometry experiments are presented to complement the SFG results.

SFG Measurements on a Static Monolayer: Density Dependence of the SFG Spectra. In the middle panel of Figure 1, SFG spectra for DPPC on H_2O are depicted at different areas per molecule (density). The density was varied by adding droplets of solution of DPPC in $CHCl_3$. The bottom spectrum is from the air−water interface and shows a signal originating from the hydrogen-bonded water molecules between 3000 and 3600 cm^{-1} and a signal from the free OH at ~3700 cm^{-1}.[20] The addition of the surfactant DPPC to the surface, surprisingly, does not result in changes in the SFG spectrum as long as the pressure remains below our detection limit. Although lipids are present on the surface, they are not detected in the SFG experiment and do not detectably influence the water structure: the SFG spectra in the absence of lipids and in the presence of DPPC at low density are indistinguishable (see bottom panel of Figure 1). Given the signal-to-noise of our SFG experiment, an intensity drop of 10% would be measurable. Since the intensity depends on the square of the number density (all other things being equal), we conclude that at most 3−4% of the free OH groups is influenced by the lipids. Remarkably, the surfactant does not affect the water structure either, especially if one realizes that the minimum area taken up by a lipid molecule (for a fully compressed monolayer) is ~40 Å^2. On a water area of 100 Å^2, there are approximately three OH molecules,[21,22] so that the area per free OH is roughly ~30 Å^2. If we assume a statistical distribution of surfactants over the surface, one would therefore expect that at a lipid density of 108 Å^2 per molecule approximately one in three free OH groups would be affected, which would make the SFG signal at the free OH drop to half of the original intensity. The surfactants also do not show up in the spectrum: no detectable CH vibrations occur between 2800 and 3000 cm^{-1} in the middle panel of Figure 1 for low density—in agreement with Roke[4] and Chen.[9] As visible in the middle panel of Figure 1, increasing the density of surfactant by adding more droplets of DPPC in chloroform results in a pressure rise and changes in the SFG spectrum: CH vibrations appear at frequencies of ~2850 (CH_2 symmetric stretch), ~2880 (CH_3 symmetric stretch), and ~2950 cm^{-1} (CH_3 Fermi resonance and CH_3 asymmetric stretch),[9,23] the water H-bonded signal increases, and the free OH peak disappears. The interfacial system effectively changes in a stepwise fashion from a water/air to a water/surfactant interface. To quantify how abrupt the spectral changes are, we measured continuously the pressure and SFG spectra while compressing the monolayer. The initial monolayer was prepared by adding drops of 0.5 μL DPPC solution until an area per molecule of ~100 Å^2 was achieved. The results for DPPC on H_2O are depicted in Figure 2a. The different curves are obtained by integrating different spectral windows from SFG spectra as is indicated by the insets

dx.doi.org/10.1021/jp2074545 | J. Phys. Chem. B 2012, 116, 2703−2712

in Figure 2a. For these experiments, the central frequency of the IR pulses was kept fixed to achieve sufficient signal strength during continuous compression. Therefore, in this experiment, we could only measure the CH vibrations of the surfactant and the H-bonded water together. The signals of the H-bonded water and the free OH bonds were measured in a subsequent run at higher IR frequency. From Figure 2a it is clear that changing the density of the surfactant by only a few percent around 85 Å^2 has a dramatic effect on the system. The very sudden rise of the CH signal has been reported before,[4,9] but the sharp changes in the water spectrum have not. The increase in the water signal seems to be a stepwise process: between roughly 85 and 50 Å^2 per DPPC molecule the SFG intensity is constant. Changing the lipid density by a factor of 1.5 has little effect on the signal strength of the water molecules in and underneath the monolayer. Like the water signal, the lipid C−H stretch intensity is also more or less constant up to ∼50 Å^2 per molecule (Figure 2). The constant SFG signal for the C−H vibration of DPPC at the plateau in the pressure isotherm has been reported in the literature.[4,9] We observed the same sharp rise of the SFG signal for DPPC upon compression under PSS and SPS polarization. Moreover, two different surfactants, palmitic acid and 1-dodecanol (see Figure 2c and d), show a similar sudden sharp rise measured under SSP polarization, although the area per molecule where the step occurs depends on the molecule (20 and 30 Å^2 per molecule, respectively). The observed behavior therefore appears to be general for surfactants: it is observed for a lipid, alcohol, and fatty acid.

BAM Measurements. To confirm that the surfactant molecules are present on the surface, we have performed Brewster Angle Microscopy (BAM) measurements of which the results are depicted in Figure 3. Already at the very low density of 140 Å^2 per molecule DPPC is visible on the surface. It is well-known that at a DPPC density below roughly 90 Å^2 per molecule the monolayer displays coexistence of the gaseous and liquid expanded phase, giving rise to dark and light patches in the BAM experiments, respectively. The amount of bright area, representing the denser liquid expanded phase, increases upon increasing the density. At 84 Å^2 per molecule the image is without any contrast showing the homogeneity in the layer on the micrometer length scales: the system is in the liquid expanded phase. A further compression of the layer (increase in density) results in small, bright, star-like domains presenting the liquid condensed phase on a dark background of the liquid expanded phase. The isotherm shows a plateau here. At the end of the plateau the pressure rises sharply, and the BAM picture is homogeneous: the entire surface is in the condensed phase. Our BAM results are in agreement with the literature.[17,24]

SFG Measurements on a Static Monolayer: Fluence Dependence of the SFG Signal. Although the BAM microscopy data show that already at 140 Å^2 per molecule the domains with lipids in the liquid expanded phase are visible, the molecules are invisible for SFG. As mentioned already in the Introduction, in the past the invisibility in the CH stretch region was assigned to curling up of the tails[4] or disordered tails.[9] However, this explanation cannot explain why the water signal is not influenced by lipids up to a density of roughly 85 Å^2 per molecule. In particular, the free OH groups should be affected by the presence of the lipid, irrespective of whether the lipid is curled or not. According to the SFG results the system behaves as water/air-like above 85 Å^2 per molecule. It seems that in the laser focus at the measurement location the surface is cleaned; all the domains with liquid expanded phase appear to be removed from the SFG laser spot. In this case, one might expect that the position of the step relative to the area per molecule will depend on the laser fluence used in the experiment. To test this hypothesis we repeated the SFG measurements using a four times lower IR power. As the beam size was kept constant, the fluence was reduced by a factor 4. As is clear from Figure 2b, the step indeed moves to lower density, higher area per molecule, and becomes less steep. The inset in panel b summarizes the fluence dependence by showing the correlation between the fluence and the area per molecule at which the SFG signal appears. Apparently the laser intensity has an effect on the appearance of the SFG signal. This explanation is also in agreement with the observation of Chen et al.[9] that the P═O signal from the headgroup is only visible at high density, because only then the lipids are present in the laser focus.

Explanations of "Cleaning" of the Surface. It can be calculated that with the used laser parameters (beam size, pulse energy, and frequency) the water interfacial region will be heated. A detailed calculation is shown in the Appendix. These calculations reveal that, for the highest pulse energies available in conjunction with regions in the infrared spectrum where absorption is very strong, the single-pulse temperature increase can amount up to 10 °C. Given the repetition rate of our laser of 1 kHz, also steady-state heating occurs due to the repetitive single-pulse heating. The resulting steady-state temperature increase can amount up to tens of °C.

As a result, a lateral and axial temperature gradient appears. The lateral temperature gradient, i.e., that along the surface, gives rise to strain along the surface, which in turn will trigger the flow of water.[25] Water will flow radially away from the center of the irradiation spot, as exemplified in Figure 4a. To conserve mass, fresh water from below will replenish the water that has flown out of the irradiation spot. In this way, a donut-shaped, circular Marangoni-type flow cell will ensue, as illustrated in Figure 4b. A similar mechanism was proposed previously by Bain et al.[26] The resulting flow cell explains why there are no lipids present in the laser focus. If the fluence is too high, the diffusive, entropic forces that drive lipids into the laser focus are insufficient to counteract the Marangoni flow of water with lipids out of the laser focus. The surface is very effectively cleaned by the laser, with fresh water appearing at the surface continuously from the bulk. As the surface density and associated surface pressure increase, a point arises where the flow is insufficiently strong to counteract the diffusive, entropic forces of the surfactants. While water may still flow underneath the lipid monolayer, the monolayer is sufficiently rigid that it remains in place. At the corresponding surfactant density, the surfactant signal suddenly appears. The appearance of such interfacial Marangoni flow cells explains why the surface looks pristine when the pressure is sufficiently low, why the surfactant signal suddenly appears with increasing pressure, and why the pressure at which the signal appears depends on the laser fluence.

Another contribution to the reduction of the local lipid density within the laser focus could result from the pressure increase upon heating the layer. The surface pressure of water will increase roughly with 0.15 mN/m K.[25] A temperature increase of 10 °C will result then in a pressure increase of 1.5 mN/m for a bare water surface. With lipids on top, most likely this pressure increase will be even larger, as an estimate of the pressure increase in just the surfactant layer amounts to around 0.15 mN/m if one assumes an ideal gas, a temperature increase

dx.doi.org/10.1021/jp2074545 | J. Phys. Chem. B 2012, 116, 2703−2712

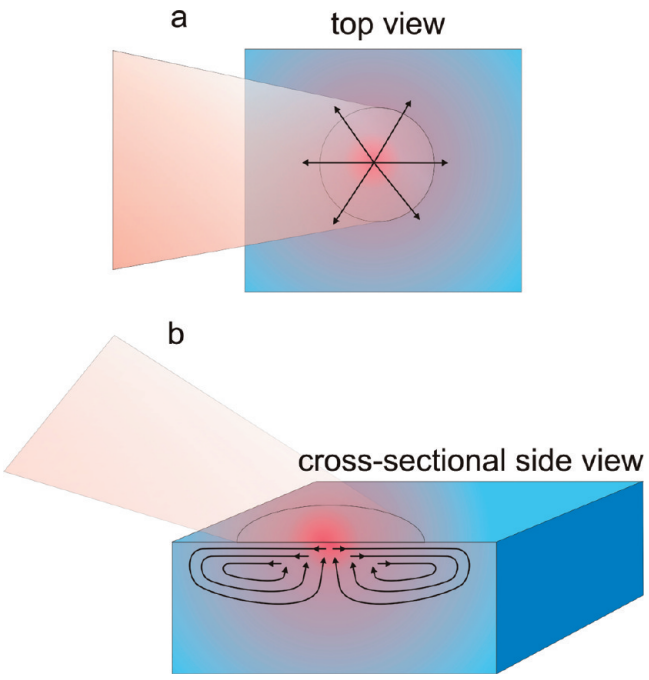

Figure 4. Schematic representation of the flow induced by the steady state heating of the near-surface region of the water sample. The temperature is schematically indicated by color, where red is hot and blue is cold. Orange shaded area shows the laser beam incident on the surface, and arrows denote the direction of the temperature gradient-induced flow. (a) Top view, showing the radial displacement of the near-surface region and (b) cross-sectional side view showing the resulting Marangoni flow cell. Note that at the center of the focus the flow of water is upward, so that the surface is effectively renewed continuously.

of 10 K, and a density of 10^{18} molecules/m^2. Clearly, the temperature increase will introduce a pressure increase. This pressure increase will result in a local expansion of the monolayer—at sufficiently low pressure the system locally may even go into the pure gaseous phase. As the unperturbed area of the trough is many orders of magnitude larger than the perturbed area, the local expansion is easily possible. At the laser spot the system is in the very low density gaseous phase with an SFG signal maybe below our detection limit. With this equilibrium thermodynamics scenario, no SFG signal is expected for the whole coexistence region of the gaseous and liquid expanded state. The system will locally reduce its pressure, and the system is at the laser spot in the full gaseous state. However, our data (Figure 2b) show that the step could already appear at the coexistence, which indicates that equilibrium thermodynamics cannot explain everything. We might also have dynamical contributions. At low IR fluence the heating is not sufficient anymore to make the phase transition to the gaseous phase.

SFG Measurements on a Moving Monolayer: Density Dependence of the SFG Spectra. To obtain the "true" surface SFG response at low surfactant densities, we performed SFG experiments in a rotating trough which are depicted in Figure 5. The sample is rotated in such a manner that at the laser focus the sample moves with a speed of ~0.06 m/s, and the steady state heating is minimal in this case. Figure 5a shows SFG spectra for the water–air interface and for 230 Å^2 per molecule DPPC while rotating the trough and not rotating it. The SFG signals for a bare water interface and a nonrotating

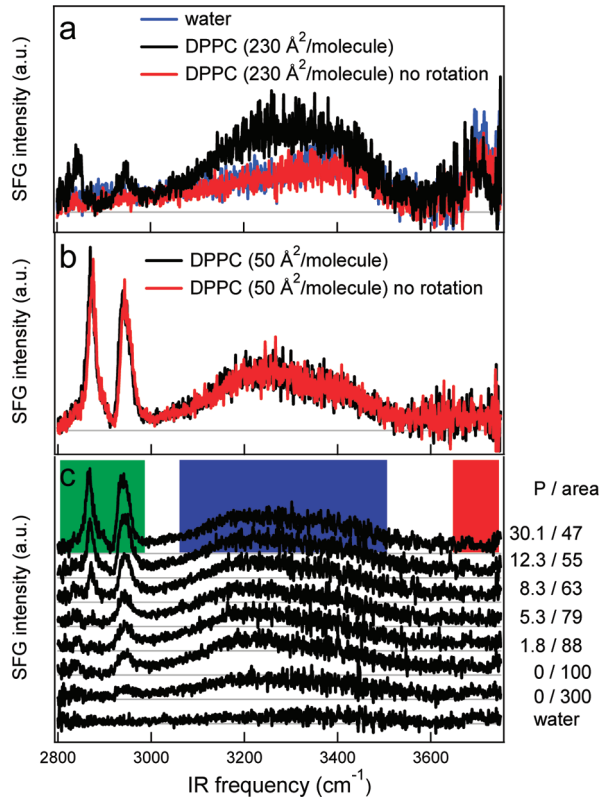

Figure 5. (a) SFG spectra in SSP polarization for DPPC on water at 230 Å^2 per molecule with (black) and without (red) rotating the trough. The sample is rotated in such a manner that at the laser focus the sample moves with a speed of ~0.06 m/s. Without rotating, the spectrum is identical to the water–air interface (blue). (b) At high density (50 Å^2 per molecule), there is no difference between rotating (black) and nonrotating (red). (c) SFG spectra (SSP polarization) for a bare water surface (bottom spectrum) and for DPPC on water with increasing density. The pressure (mN/m) and area per molecule (Å^2), increasing and decreasing, respectively, from bottom to top are given next to the graph. The area per molecule has been controlled by the amount of droplets of chloroform solution. The colored squares mark the area of integration used for Figure 6. A relative low IR fluence (1.5 mJ/cm^2) was used in this experiment.

trough are identical. By rotating the trough, a CH signal appears, and the water signal increases. The appearance of the signal is a delicate balance between the rotation speed and the IR fluence. To obtain a low enough IR fluence (~1.5 mJ/cm^2) we used a relative unfocused IR beam (beam waist ~500 μm) in this experiment. At a too low rotation speed, still no SFG signal is visible; the laser-induced flow that serves to repel lipids from the focus is still too high. At high density the signal shape and strength are independent of whether the trough is rotating or not (Figure 5b). Figure 5c depicts SFG spectra for increasing density (from bottom to top) of DPPC on water while continuously rotating the trough. The lipid density has been controlled by adding drops of DPPC in chloroform. The bottom spectrum is for the air–water interface. Clearly, the CH and H-bonded OH signals increase slowly and continuously as the DPPC density increases, while the free OH signal decreases smoothly as well.

The integrated SFG intensities for the different vibrations in the SFG spectrum are plotted together with the surface pressure in Figure 6a as a function of the area per molecule. The CH intensity increases in a nonlinear fashion with the

dx.doi.org/10.1021/jp2074545 | J. Phys. Chem. B 2012, 116, 2703–2712

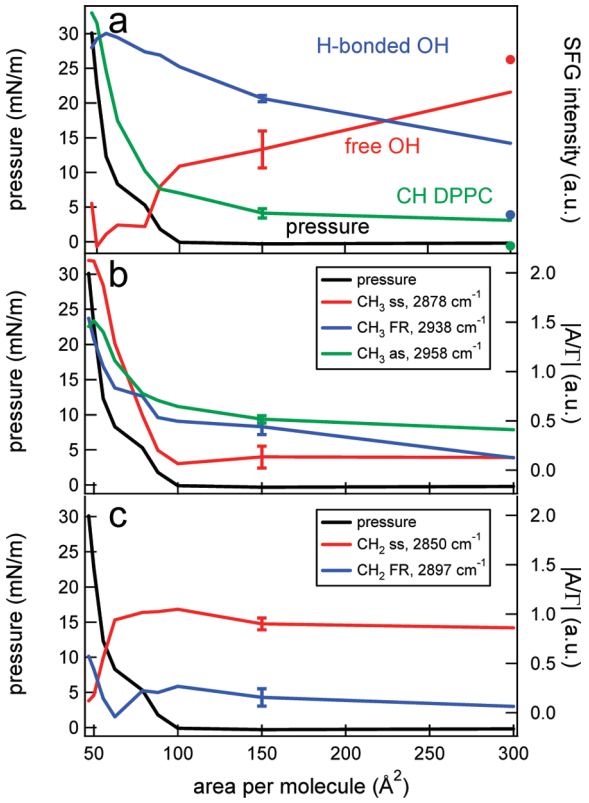

Figure 6. (a) Surface pressure (black, left axis) and integrated SFG intensity (right axis) for the CH signal of DPPC (green), the H-bonded OH signal (blue), and the free OH signal (red) as a function of the area per molecule. The data points are obtained by integrating specific spectral regions, marked by the colored squares, in the spectra from Figure 5. The CH, OH, and free OH areas of a pure water layer, measured just before spreading the surfactant, are given as green, blue, and red dots, respectively. The integrated SFG signals have been normalized and slightly offset with respect to each other for clarity. (b) Surface pressure (black, left axis) and the absolute amplitude/bandwidth ratios ($|A/\Gamma|$) of the different CH_3 resonances (right axis), obtained by fitting the data of Figure 5 with a Lorenztian line shape model. (c) Like b, but for the CH_2 resonances. Typical error bars are indicated in the graphs.

amount of DPPC molecules present on the surface. The water signal continuously increases, while the free OH signal continuously decreases with increasing amount of molecules at the surface and, as expected,[27] reaches zero value when the system reaches the liquid expanded phase. In principle, in the coexistence region of the gaseous and liquid expanded phase (above ~100 Å^2 per molecule), one might expect to see a fluctuating SFG signal because the gaseous phase does not give a signal, while the liquid expanded phase does. Such fluctuating signals have been observed with second harmonic generation[28] and ellipsometry.[29] However, these fluctuations are not observed here as the presented SFG spectra are averaged over 10 min which is long on the time scale of the diffusion of the domains, which happens on time scales of tens of seconds.[28,29]

Different SFG Spectra at High Density As a Function of Laser Fluence. By comparing two SFG spectra (Figure 7) of a lipid layer at high pressure (high lipid density), measured at different fluences, a difference is observed at the CH peaks, while the water band is more or less the same. At the relatively high fluence (bottom panel) of ~10 mJ/cm^2, the CH_2 peak at

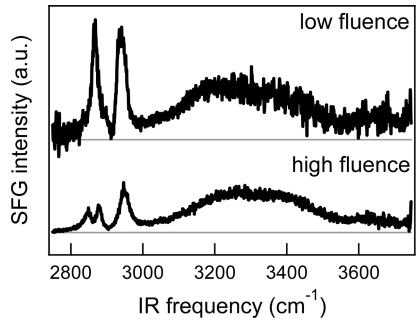

Figure 7. SFG spectra (SSP polarization) for DPPC on water at high density (~45 Å^2 per molecule) at low (~1.5 mJ/cm^2) and high fluence (~10 mJ/cm^2), respectively, for which the single pulse heating amounts to between 0.3 and 3 °C (depending on the IR frequency) and between 2 and 19 °C, respectively. The spectra are offset for clarity and are scaled to the relative IR intensities. Note the very different shape, as a result of thermal effects occurring at high fluence. Both spectra were measured with a nonrotating trough.

2850 cm^{-1} is still clearly visible, while this peak is absent in the top panel for low fluence (~1.5 mJ/cm^2). Also, in the high fluence spectrum the intensity of the CH_3 peaks (2880 and 2950 cm^{-1}) is low relative to the water, in contrast to the low-fluence measurement. These two observations are a clear indication that at high fluence the monolayer is affected by the laser: due to the heat the tails are more disordered resulting in more gauche defects and therefore the presence of the CH_2 peak and a weakening of the CH_3 signal. Apparently, the repetitive excitation with the laser induced a phase transition from the gel state with ordered tails to the liquid crystalline state with less ordered tails.[30] As the experiments were performed at room temperature (~23 °C) and the phase transition temperature is 41 °C,[30] we can conclude that the steady state heating of the sample is at least 18 °C in the high fluence case, which is not unreasonable given the single shot temperature rise estimated to be between 2 and 19 °C (depending on the IR frequency) based on the focus size and the penetration depth of the IR light (see the Appendix). For the low fluence case (top panel), the steady state temperature rise does not exceed 18 °C, as we still see ordered tails indicating the gel state also by stopping the rotation of the trough.

Moreover, the thermal effect of the laser is already visible in the spectrum in Figure 1 taken at an area per molecule of 78 Å^2, where, remarkably, a large signal is present in the O−H but not in the C−H stretch region. This can be traced to variations in the IR laser intensity by scanning across the C−H and O−H stretch regions: at low frequencies the IR intensity is higher than at high frequencies, resulting in an accumulation of more heat at the interface in the C−H region than in the O−H region (see the Appendix). Note that thermal diffusion in between laser shots occurs over large length scales compared to the penetration depth, so that only the laser intensity (and not the penetration depth) is relevant for the steady state temperature increase (see Appendix, Figure 9). As soon as the infrared source reaches low frequency (C−H region), the lipids are transported away more efficiently due to the flow because of the larger thermal gradient. If the infrared frequency is slightly higher the accumulated heat is slightly less, and the domains can be detected. This explains the presence of the water signal but the absence of the CH signal. In line with the observation of Casson et al.[26] in experiments with a

dx.doi.org/10.1021/jp2074545 | J. Phys. Chem. B 2012, 116, 2703−2712

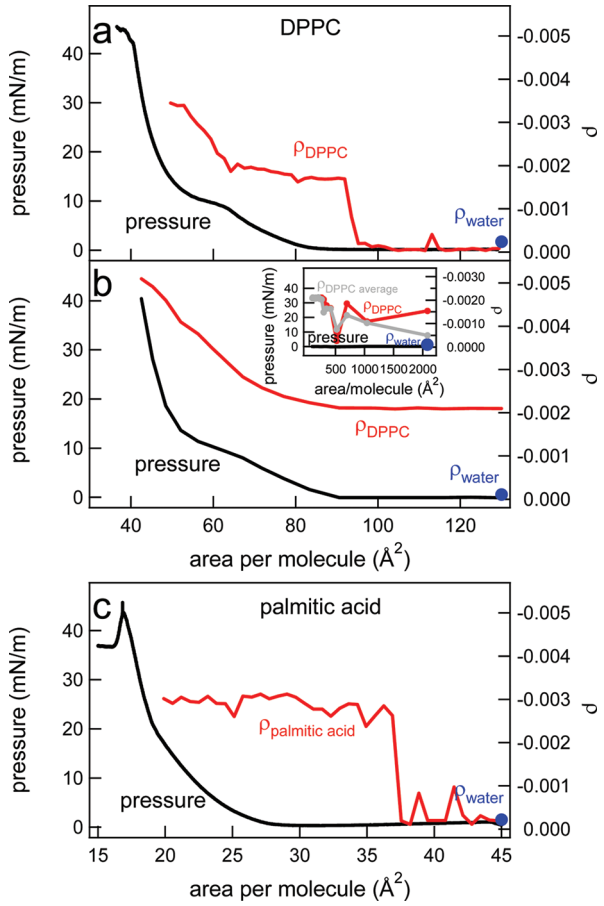

Figure 8. (a) Surface pressure (black, left axis) and the coefficient of ellipticity (red, right axis) for DPPC on water during continuously compressing the monolayer after preparation of the monolayer by quickly adding DPPC solution until an area per molecule of 130 Å^2 has been reached. (b) Surface pressure (black, left axis) and the coefficient of ellipticity (red, right axis) for DPPC on water as a function of the area per molecule. The area was changed by adding more DPPC in a drop by drop fashion with a few minutes between each drop. The lowest area per molecule reached in this way is 2000 Å^2 per molecule. The inset shows the coefficient of ellipticity (for one particular experiment (red) and the average of three experiments (gray)) and the pressure at very low density. (c) Surface pressure (black, left axis) and the coefficient of ellipticity (red, right axis) for palmitic acid on water during continuously compressing the monolayer after preparation of the monolayer by quickly adding a solution of palmitic acid until an area per molecule of 45 Å^2 has been reached. The ellipticity of pure water, measured just before spreading the surfactant, is given as a blue dot in each panel.

nanosecond IR laser, our data show that by using high intensity femtosecond IR lasers experimental care has to be taken for distortion of results due to sample heating. In both cases, steady state heating is mainly responsible for the observed distortions, and therefore only the laser fluence is important.

Ellipsometry. Interestingly, in ellipsometry a step in the coefficient of ellipticity has repeatedly been observed when compressing the layer at low densities (near-zero pressure) for both lipids and fatty acids.[14−18] The same is observed here: in Figure 8a the coefficient of ellipticity as a function of area per molecule for DPPC is depicted together with the simultaneously measured surface pressure. The reflectivity at 130 Å^2 per molecule is comparable to that for a water−air interface. Upon compressing the monolayer after initially making the

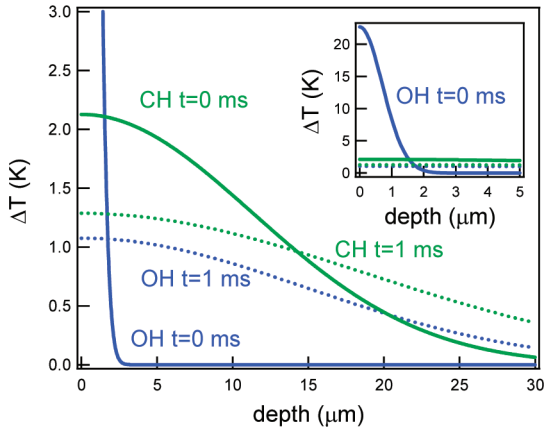

Figure 9. Temperature increase as a function of depth into the water layer for the IR beam in resonance with the CH (green) or OH (blue) vibration. The solid and dotted line are for t = 0 and t = 1 ms, respectively. The inset shows the same graph but with an expanded y-axis.

layer by adding drops of chloroform solution until an area per molecule of 130 Å^2, a similar step as in the SFG data has been observed, but the step appears at different area per molecule, 95 vs 85 Å^2. For palmitic acid, a step is observed with ellipsometry at ∼37 Å^2 per molecule (Figure 8c), as opposed to the SFG experiments where it occurs at 20 Å^2 per molecule (Figure 2c). In contrary to the SFG experiments, the laser used in the ellipsometry experiments is not in resonance with a molecular transition, and the fluence of the laser is very low, so that Marangoni flow cells appearing as a result of heating effects can be excluded as a cause for the step in the signal. The temperature increase, calculated using the same expressions as given in the Appendix for the IR, is below 0.001 °C in 1 s. Remarkably, if the ellipsometry experiment is performed in a different way, not under continuous compression but by changing the area by adding more DPPC solution, the coefficient of ellipsometry behaves very differently (Figure 8b): The discontinuity in the ellipticity coefficient is absent. We note that, in contrast to these ellipsometry results, the SFG results were independent of the manner in which the monolayer was prepared. For the ellipsometry, already at very low density, even after adding the first drop of DPPC solution, the coefficient of ellipticity clearly differs from that of pure water. Up to roughly 300 Å^2 per molecule the value is fluctuating because liquid-expanded domains of a size comparable to that of the laser spot are floating around. One might expect that upon averaging multiple experiments the coefficient will increase linearly with density in this regime where we see fluctuations for one experiment. Indeed, as can be seen from the gray line in the inset of Figure 8b, an average of three experiments approaches this linear relationship. At higher density, from ∼300 to 90 Å^2 per molecule where the system is still in a coexistence of gaseous and liquid expanded phase, the coefficient of ellipticity is flat. At lower density, it rises in a similar way as observed under compression (Figure 8a). The main difference between the two types of experiments is the time that the system is allowed to relax and equilibrate. In the first experiment, under continuous compression, the layer is made by quickly adding DPPC solution until the area per molecule reaches 130 Å^2 per molecule. In the second experiment, the layer is a few minutes at 2000 Å^2 per molecule, then a few minutes at 1000 Å^2 per molecule, and so on.

dx.doi.org/10.1021/jp2074545 | J. Phys. Chem. B 2012, 116, 2703−2712

Ducharme et al.[14] have previously observed that the onset of the plateau at low density in a compression experiment depends on the initial surface density. They suggested that at low initial density the molecules have space to orient resulting in a layer that is active in ellipsometry; i.e., the molecules are aligned and oriented under a similar angle with respect to the surface normal.[14] If the initial concentration is too high, the molecules are constrained in their motion due to lack of space and get stuck in a metastable state that exhibits no or only very little interfacial birefringence, to which ellipsometry is very sensitive. At high initial densities, the intermolecular interactions within the surfactant layer apparently prevent ordered alignment of the lipid molecules. The critical area per molecule is expected to be approximately 300 Å^2 per molecule, the area for a flat-lying DPPC molecule. For this initially kinetically frozen monolayer that does not provide any contrast in ellipsometry, significant intermolecular interactions (that become more important as the monolayer is compressed) are required to induce collective alignment of the lipid molecules. Our observations are perfectly consistent with the hypothesis of Ducharme et al.: for the slowly prepared layer, the onset of the plateau is at the low density (high area per molecule) of around 250 Å^2 per molecule, while for the layer with the initial surface coverage at 130 Å^2 per molecule the step appears at much higher density. Interestingly, the coefficient of ellipsometry remains constant from roughly 300 Å^2 per molecule until the moment the pressure starts to rise at roughly 90 Å^2 per molecule. Although the density in the coexistence of gaseous and liquid expanded phase changes by a factor of 3, the coefficient is fully flat. However, the BAM results show that more liquid expanded phase (the domains get larger) is occurring by compressing the layer. These results can only be brought in agreement with each other if the effective refractive index or the thickness of the layer decreases. Fitting of the SFG results obtained with the rotating trough (Figure 5) with a Lorentzian line shape model (see, e.g., ref 4) shows that in the same density regime where the coefficient of ellipsometry is constant the amplitude of the CH_2 symmetric stretch vibration is flat as well. The results of the fit are depicted in Figure 6b and 6c. Although the lipid density increases, the average number of gauche defects remains constant, indicating that the layer changes orientation. Apparently the layer does that in such a way that both the coefficient of ellipsometry and the SFG signals of the CH_2 symmetric stretch vibration remain constant.

Although both ellipsometry and SFG show a discontinuity in their signal before or around the surfactant density at which the pressure starts to rise, the origin appears to be different. In SFG measurements, the step is related to the heating of the water phase. Due to this heating a net flow of surfactants out of the laser focus will occur, as illustrated in Figure 4. At low surfactant density, the surface is cleaned in the laser focus: all the lipid molecules are effectively removed from the SFG laser spot. We would like to stress that a very low fluence of the resonant IR laser (less than 3 °C temperature increase per pulse with the IR at the maximum of the OH band) is already sufficient to displace the domains with surfactants out of the focus as indicated in Figures 2 and 5. At higher surfactant density the repelling laser force does no longer win from the diffusion force driving the molecules into the laser focus. The density where this occurs, and thus where the SFG signal appears, depends on the type of surfactant in a similar way as the isotherm. The earlier, upon compression, the pressure deviates from zero, the earlier in a compression isotherm the step from no SFG signal to a signal is observed. We would like to emphasize that only by refreshing the sample in between laser pulses by using a rotating trough, the step observed in an SFG experiment can be fully eliminated. Only then the steady state heating is low enough to avoid repelling of the domains out of the laser focus. With the rotating trough, the "true" SFG spectrum can be measured already at very low density.

In ellipsometry, the laser does not disturb the layer to the same extent because the peak power is much lower and the radiation is not in resonance with a molecular transition. The step in ellipsometry has its origin in a metastable state that occurs when the initial lipid density is too high. For such a system, it takes significant compression to induce the molecular transition from the invisible disordered state to a visible state with collectively aligned tails. However, the density where this step takes place depends on the preparation of the layer. The step is even completely absent if the layer is prepared by allowing the molecules sufficient space and time to relax. The transition from not aligned to aligned tails, responsible for the step in ellipsometry, can not explain the observed behavior in the SFG case because the water signal, both the hydrogen bonded and the free OH, should not show a step if the tails of the surfactants align.

■ CONCLUSION

We have elucidated the origin of the sudden increase in signal observed in SFG experiments for surfactant monolayers on water as a function of surfactant density. We demonstrate, by measuring the water signal, that surfactants are displaced from the probed region by the laser pulses. The use of a rotating trough avoids the steady state heating of the sample causing photocleaning and makes the sample spatially homogeneous. This allows the measurement of "true" SFG spectra in the CH and OH region of DPPC on water over the whole density range. The presence of CH_2 vibrations in the spectrum in the liquid expanded phase shows that the tails of the molecules are not well ordered. In the liquid condensed phase only vibrations originating from the CH_3 groups are present: the lipids are ordered without gauche defects. The water signal increases continuously until the liquid condensed phase is reached. The free OH peaks, representing water molecules without DPPC on top, decrease until no gaseous phase is present anymore. If a nonrotating trough is used, no SFG signal is detected up to very high densities because the liquid expanded phase domains are readily removed from the laser spot by the same laser. Brewster angle microscopy which shows the domains, in combination with an infrared laser beam, might be able to visualize the effect of steady state heating.

■ APPENDIX

The single shot temperature rise can be calculated from the beam size and the absorption cross-section at a given frequency. According to ref 31 the Lambert absorption coefficient is $\alpha(\lambda) = 4\pi k(\lambda)/\lambda$, where λ is the wavelength of light and k the imaginary part of the refractive index. For an infrared laser beam with a frequency of 3100 cm^{-1}, α is 0.36 μm^{-1}. Neglecting the roughly 1% reflection of the light from the surface, and considering that from the original transmitted intensity I_0 the remaining intensity I at distance l from the point of incidence scales as $I/I_0 = e^{-\alpha * l}$, the average absorbed power in the interfacial region where 50% of the IR light is absorbed from the laser pulse can be readily calculated.

dx.doi.org/10.1021/jp2074545 | J. Phys. Chem. B 2012, 116, 2703−2712

Specifically, with the details given in the Experimental Section about the IR beam (power: 6 μJ; beam waist: 200 μm; angle of incidence: 40°) for the high fluence case (Figures 1, 2 (except Figure 2b), and 7 bottom panel) and the heat capacity of water (4.2 J/gK), we obtain a single shot temperature increase of 9 K averaged over the volume formed by the beam size of the laser at the surface and the 50% penetration depth. At the peak of the water absorption (at ~3300 cm^{-1} with ~4 μJ IR), the rise is even 19 K with a 50% penetration depth of 0.6 μm, while at the CH region (at ~2940 cm^{-1} with ~6 μJ IR) the rise is 2 K with a 50% penetration depth of 10 μm. For the low fluence case (Figures 5, 6, and 7, top panel) the beam waist is roughly 2.5 times larger, resulting in a roughly 6 times lower fluence. The single shot temperature jumps are therefore also 6 times lower.

The same calculation for the visible beam reveals that the visible beam is not relevant for the heating process: the single shot temperature increase for the visible beam is only 0.06 mK and therefore negligible.

The effects described in the current paper are, however, not caused by a single shot but by steady state heating. Given the thermal diffusion coefficient of water being 1.11×10^{-3} cm^2/s and assuming one-dimensional diffusion of heat perpendicular to the water surface, one can calculate that in 1 ms (the time between two laser shots) the heat diffuses roughly 20 μm away from the interface. More precisely, at 1 ms after the pulse hits the surface, the heat has a Gaussian distribution with a half width half-maximum at ~20 μm. As the IR penetration depth is at all our frequencies smaller than the diffusion length of 20 μm, the distribution of heat at 1 ms is more or less frequency independent. Therefore, the heat at the surface at 1 ms is predominantly determined by the IR power which is higher at low frequencies (i.e., at the C−H region) resulting in more steady state heat at low frequencies. The heat distributions obtained from such calculations are depicted in Figure 9 for two different times after excitations at the CH and OH vibration.

AUTHOR INFORMATION

Notes

The authors declare no competing financial interest.

ACKNOWLEDGMENTS

This work is part of the research program of the "Stichting voor Fundamenteel Onderzoek der Materie (FOM)", which is financially supported by the "Nederlandse organisatie voor Wetenschappelijk Onderzoek (NWO)". The authors thank Remco Fokkink and Marc-Jan van Zadel for help with the ellipsometry experiments and are very grateful to Ron Shen, Colin Bain, and Harald Pleiner for many helpful discussions.

REFERENCES

(1) Sefler, G. A.; Du, Q.; Miranda, P. B.; Shen, Y. R. *Chem. Phys. Lett.* **1995**, *235*, 347−354.
(2) Conboy, J. C.; Messmer, M. C.; Richmond, G. L. *J. Phys. Chem. B* **1997**, *101*, 6724−6733.
(3) Zhuang, X.; Miranda, P. B.; Kim, D.; Shen, Y. R. *Phys. Rev. B* **1999**, *59*, 12632−12640.
(4) Roke, S.; Schins, J.; Müller, M.; Bonn, M. *Phys. Rev. Lett.* **2003**, *90*, 128101.
(5) Watry, M. R.; Tarbuck, T. L.; Richmond, G. L. *J. Phys. Chem. B* **2003**, *107*, 512−518.
(6) Ma, G.; Allen, H. C. *Langmuir* **2006**, *22*, 5341−5349.
(7) Tyrode, E.; Johnson, C. M.; Rutland, M. W.; Claesson, P. M. *J. Phys. Chem. C* **2007**, *111*, 11642−11652.
(8) Ohe, C.; Arai, M.; Kamijo, H.; Adachi, M.; Miyazawa, H.; Itoh, K.; Seki, T. *J. Phys. Chem. C* **2008**, *112*, 6359−6365.
(9) Chen, X.; Allen, H. C. *J. Phys. Chem. A* **2009**, *113*, 12655−12662.
(10) Nihonyanagi, S.; Yamaguchi, S.; Tahara, T. *J. Chem. Phys.* **2009**, *130*, 204704.
(11) Sovago, M.; Vartiainen, E.; Bonn, M. *J. Chem. Phys.* **2009**, *131*, 161107.
(12) Chen, X.; Hua, W.; Huang, Z.; Allen, H. C. *J. Am. Chem. Soc.* **2010**, *132*, 11336−11342.
(13) Ma, G.; Chen, X.; Allen, H. C. *J. Am. Chem. Soc.* **2007**, *129*, 14053−14057.
(14) Ducharme, D.; Max, J. J.; Salesse, C.; Leblanc, R. M. *J. Phys. Chem.* **1990**, *94*, 1925−1932.
(15) Hönig, D.; Möbius, D. *J. Phys. Chem.* **1991**, *95*, 4590−4592.
(16) Petrov, J. G.; Pfohl, T.; Möhwald, H. *J. Phys. Chem. B* **1999**, *103*, 3417−3424.
(17) Miñones, J.; Patino, J. M. R.; Conde, O.; Carrera, C.; Seoane, R. *Colloids Surf. A: Physicochem. Eng. Aspects* **2002**, *203*, 273−286.
(18) Pérez-Morales, M.; Pedrosa, J. M.; Muñoz, E.; Martín-Romero, M. T.; Möbius, D.; Camacho, L. *Thin Solid Films* **2005**, *488*, 247−253.
(19) Hénon, S.; Meunier, J. *Rev. Sci. Instrum.* **1991**, *62*, 936−939.
(20) Du, Q.; Superfine, R.; Freysz, E.; Shen, Y. R. *Phys. Rev. Lett.* **1993**, *70*, 2313−2316.
(21) Du, Q.; Freysz, E.; Shen, Y. R. *Science* **1994**, *264*, 826−828.
(22) Wang, Y.; Hodas, N. O.; Jung, Y.; Marcus, R. A. *Phys. Chem. Chem. Phys.* **2011**, *13*, 5388−5393.
(23) Ji, N.; Ostroverkhov, V.; Chen, C.-Y.; Shen, Y.-R. *J. Am. Chem. Soc.* **2007**, *129*, 10056−10057.
(24) Lucero, A.; Niño, M. R. R.; Gunning, A. P.; Morris, V. J.; Wilde, P. J.; Patino, J. M. R. *J. Phys. Chem. B* **2008**, *112*, 7651−7661.
(25) Probstein, R. F. *Physicochemical Hydrodynamics*, 2nd ed.; Wiley: New York, 1994.
(26) Casson, B. D.; Braun, R.; Bain, C. D. *Faraday Discuss.* **1996**, *104*, 209−229.
(27) For the free OD, Ma et al. (ref 13) observed that the decrease of the peak at 2750 cm^{-1} coincides with a new peak appearing at roughly 2700 cm^{-1} upon compressing the monolayer. While we could reproduce this observation for the free OD stretch, for the free OH we observe a decrease of the free OH intensity to zero as soon as the system reaches the liquid expanded phase, without the appearance of a resonance at lower frequency.
(28) Zhao, X.; Goh, M. C.; Subrahmanyan, S.; Eisenthal, K. B. *J. Phys. Chem.* **1990**, *94*, 3370−3373.
(29) Rasing, T.; Hsiung, H.; Shen, Y. R.; Kim, M. W. *Phys. Rev. A* **1988**, *37*, 2732−2735.
(30) Lewis, R. N. A. H.; Mak, N.; McElhaney, R. N. *Biochemistry* **1987**, *26*, 6118−6126.
(31) Hale, G. M.; Querry, M. R. *Appl. Opt.* **1973**, *12*, 555−563.